

Looseness localization for bolted joints using Bayesian operational modal analysis and modal strain energy

Advances in Mechanical Engineering
2018, Vol. 10(11) 1–10
© The Author(s) 2018
DOI: 10.1177/1687814018808698
journals.sagepub.com/home/ade


Yu-Jia Hu¹, Wei-Gong Guo¹, Cheng Jiang² , Yun-Lai Zhou³ and Weidong Zhu⁴

Abstract

Bayesian operational modal analysis and modal strain energy are employed for determining the damage and looseness of bolted joints in beam structures under ambient excitation. With this ambient modal identification technique, mode shapes of a damaged beam structure with loosened bolted connections are obtained based on Bayesian theory. Then, the corresponding modal strain energy can be calculated based on the mode shapes. The modal strain energy of the structure with loosened bolted connections is compared with the theoretical one without bolted joints to define a damage index. This approach uses vibration-based nondestructive testing of locations and looseness of bolted joints in beam structures with different boundary conditions by first obtaining modal parameters from ambient vibration data. The damage index is then used to identify locations and looseness of bolted joints in beam structures with single or multiple bolted joints. Furthermore, the comparison between damage indexes due to different looseness levels of bolted connections demonstrates a qualitatively proportional relationship.

Keywords

Looseness localization, bolted joints, damage detection, Bayesian operational modal analysis, modal strain energy

Date received: 5 April 2018; accepted: 24 September 2018

Handling Editor: Magd Abdel Wahab

Introduction

Structures often suffer issues of accumulated damages due to changes in loadings and deterioration from age or environmental factors. Damage detection is therefore a key step in structural health monitoring.¹ Assessment of the state of a structure has been conducted by using either direct visual inspection or experimental techniques such as acoustic emission, ultrasonic check, and magnetic particle inspection to avoid causing destruction or influences to structural operation.² A characteristic of all these local methodologies is that they require a priori localization of damaged zones and lack practicability for large-scale structures.

These limitations can be resolved by using vibration-based (VB) methods, which can give a global damage assessment. Bayesian operational modal analysis

(BOMA)^{3–10} is more convenient than experimental modal analysis (EMA) or conventional operational modal analysis (OMA) methods because it can process

¹School of Mechanical Engineering, University of Shanghai for Science and Technology, Shanghai, China

²Department of Civil and Environmental Engineering, The Hong Kong Polytechnic University, Kowloon, Hong Kong

³Department of Civil & Environmental Engineering, National University of Singapore, Singapore

⁴Department of Mechanical Engineering, University of Maryland, Baltimore, MD, USA

Corresponding author:

Cheng Jiang, Department of Civil and Environmental Engineering, The Hong Kong Polytechnic University, Kowloon, Hong Kong.
Email: c.jiang@polyu.edu.hk



the response histories at all the measured degrees of freedom (DOFs) and only one set of response time histories is required.^{3,4} Moreover, it has good robustness against noisy measurement data because it uses directly calculated fast Fourier transform (FFT) results without the need of smoothing or averaging data.^{5,6} Thus, such method gives a great implication for the economy and convenience to identify dynamic responses of structures under their actual working situations. And the identification accuracy of the global damage can be validated.

Nowadays, many structural damage identification methods based on dynamic responses and dynamic parameters, including model updating methods, neural network methods, sensitivity-based methods, and damage index (DI) identification methods,^{11–20} have been developed by comparing vibration information before and after damages to determine structural damage locations as well as assessing damage levels. Among them, DI identification methods are of increasing interest because they do not need to solve structural parameters by inversion but directly use vibration characteristics. Such methods only involve simple calculations and easy implementations and, hence, can generally satisfy requirements of monitoring systems.

In this work, the BOMA and modal strain energy (MSE) methods are used for identifying the locations and looseness of bolted joints in beam structures with different boundary conditions under ambient excitation. Advantages of the BOMA and MSE methods are integrated in this work. Modal parameters of beam structures with bolted joints before and after damages are determined by the BOMA method under ambient excitation. Then, by using mode shape curvature to obtain MSE, the DI can be obtained to identify locations and looseness of bolted joints in beam structures with single or multiple bolted joints. Furthermore, the comparison between DIs due to different looseness levels of the bolted connections demonstrates a qualitatively proportional relationship.

BOMA

Let θ be modal parameters including the natural frequency f , modal damping ratio ζ , mode shape Φ , power spectral density (PSD) of the modal force S , and PSD of prediction error S_e . Let $\{\mathbf{Z}_k\} = [\mathbf{F}_k^T, \mathbf{G}_k^T]^T \in R^{2n}$ be an augmented vector of the real and imaginary parts of the FFT, where \mathbf{F}_k and \mathbf{G}_k denote real and imaginary parts of the FFT, respectively.³ With a large amount of data, \mathbf{Z}_k follows a Gaussian distribution with zero mean and its covariance matrix is

$$\mathbf{C}_k = \frac{1}{2} \begin{bmatrix} \Phi \text{Re} \mathbf{H}_k \Phi^T & -\Phi \text{Im} \mathbf{H}_k \Phi^T \\ \Phi \text{Im} \mathbf{H}_k \Phi^T & \Phi \text{Re} \mathbf{H}_k \Phi^T \end{bmatrix} + \frac{S_e}{2} \mathbf{I}_{2n} \quad (1)$$

where $\Phi = [\Phi_1, \dots, \Phi_m] \in R^{n \times m}$ is the mode shape matrix, $\mathbf{I}_{2n} \in R^{2n \times 2n}$ is an identity matrix, and \mathbf{H}_k is the spectral density matrix of modal response with its (i, j) element given by

$$\mathbf{H}_k(i, j) = S_{ij} f_k^{-4} [(\beta_{ik}^2 - 1) + i(2\zeta_i \beta_{ik})]^{-1} [(\beta_{jk}^2 - 1) - i(2\zeta_j \beta_{jk})]^{-1} \quad (2)$$

with $\beta_{ik} = f_i/f_k$, in which f_i , ζ_i , and f_k are the natural frequency, damping ratio of the i th mode and Nsubk frequency with FFT results, respectively, and S_{ij} is the cross spectral density between the i th and j th modal excitations.

In Bayes' theorem, the posterior probability density function (PDF) of θ given the FFT data of output vibration is expressed as

$$p(\theta|\{\mathbf{Z}_k\}) \propto p(\theta)p(\{\mathbf{Z}_k\}|\theta) \quad (3)$$

where $p(\theta)$ is the prior PDF of θ . By assuming a noninformative prior distribution, the posterior PDF of θ , that is, $p(\theta|\{\mathbf{Z}_k\})$, is proportional to the likelihood function $p(\{\mathbf{Z}_k\}|\theta)$

$$\begin{aligned} p(\theta|\{\mathbf{Z}_k\}) &\propto p(\{\mathbf{Z}_k\}|\theta) \\ &= (2\pi)^{-(N_g-1)/2} \left[\prod_k \det \mathbf{C}_k(\theta) \right]^{-1/2} \\ &\times \exp \left[-(1/2) \sum_k \mathbf{Z}_k^T \mathbf{C}_k(\theta)^{-1} \mathbf{Z}_k \right] \end{aligned} \quad (4)$$

For convenience, the negative log-likelihood function $L(\theta)$ is used

$$p(\theta|\{\mathbf{Z}_k\}) \propto \exp[-L(\theta)] \quad (5)$$

where $L(\theta) = (1/2) \sum_k \ln \det \mathbf{C}_k(\theta) + (1/2) \sum_k \mathbf{Z}_k^T \mathbf{C}_k(\theta)^{-1} \mathbf{Z}_k$. Minimizing $L(\theta)$, which is equivalent to maximizing $p(\theta|\{\mathbf{Z}_k\})$, one can obtain the most probable values (MPVs) of the modal parameters θ . The detailed computation procedure can be found in Au et al.⁴

MSE

Physical damages of structures can cause changes to their dynamic characteristics. The vibration parameters employed in the identification of damages include the natural frequency, mode shape, damping ratio, mode shape curvature, MSE, and the flexibility matrix. Generally speaking, structural damage would reduce the stiffness, increase the damping ratio, and change the information of the frequency and mode shape.^{21,22} The MSE method involving curvatures of the mode shapes has a good sensitivity in small structural

damage identification and change of mechanical performance.^{14–16}

For a Euler–Bernoulli beam, the strain energy can be expressed as

$$U = \int \frac{EI}{2} \left(\frac{d^2y}{dx^2} \right)^2 dx \quad (6)$$

where x is along the direction of the beam length, y is the transverse displacement, EI is the bending stiffness, and d^2y/dx^2 denotes the approximated curvature of the beam. For a particular mode shape φ_k , the energy associated with the mode shape is expressed as

$$U_k = \int \frac{EI}{2} \left(\frac{d^2\varphi_k}{dx^2} \right)^2 dx \quad (7)$$

As the schematic diagram shows in Figure 1, grid points $x_1, x_2, \dots, x_i, \dots, x_n$ separate the beam to be $n - 1$ elements. Hence, the element MSE of the k th mode is given by

$$U_{k,i} = \int_{x_i}^{x_{i+1}} \frac{EI}{2} \left(\frac{d^2\varphi_k}{dx^2} \right)^2 dx \quad (8) \quad \text{and}$$

Obviously, the total MSE of the k th mode of the beam is $U_k = \sum_{i=1}^{n-1} U_{k,i}$. A participation factor of MSE associated with the i th element in the k th mode is defined as

$$F_{k,i} = U_{k,i}/U_k \quad (9)$$

The summation of all fractional energies is $\sum_{i=1}^{n-1} F_{k,i} = 1$. Similarly, φ_k^* represents the k th mode shape of the damaged structure. The corresponding total MSE and element MSE of the k th mode of the beam is expressed as U_k^* and $U_{k,i}^*$; hence, a fractional energy of the k th mode of the beam can be obtained as

$$F_{k,i}^* = U_{k,i}^*/U_k^* \quad (10)$$

Considering all measured modes m , DI β_i of the i th element is defined as

$$\beta_i = \frac{\sum_{k=1}^m F_{k,i}^*}{\sum_{k=1}^m F_{k,i}} \quad (11)$$

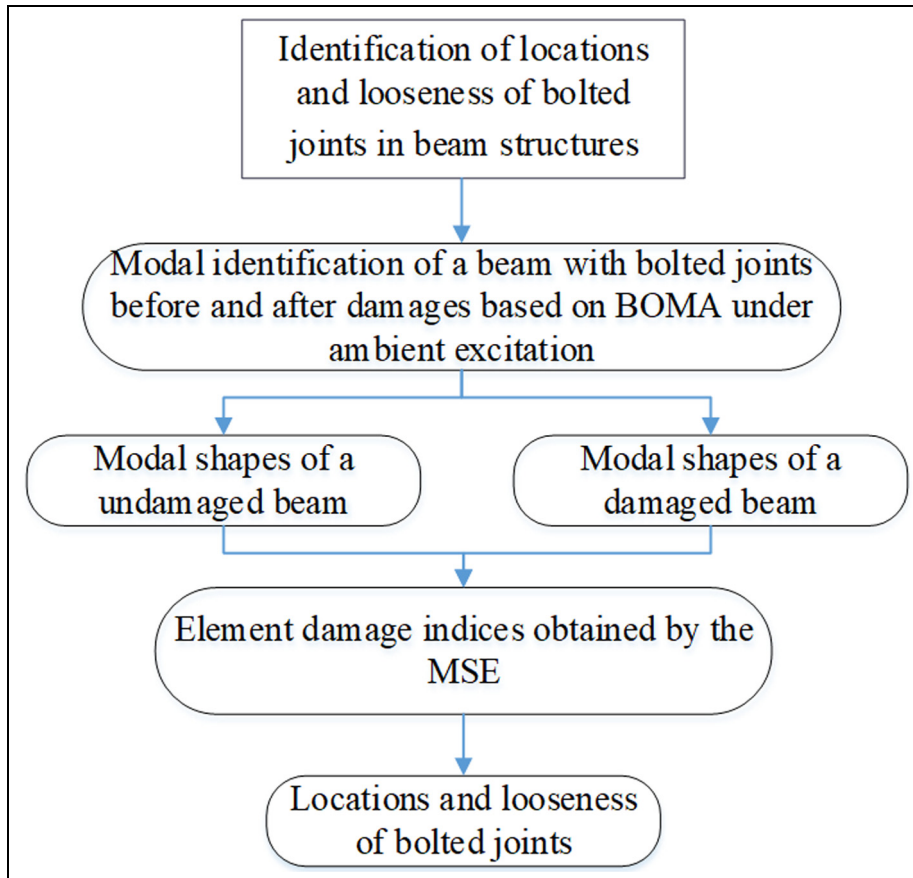


Figure 1. A flowchart of damage detection of a beam with bolted joints.

$$Z_i = \frac{(\beta_i - \bar{\beta}_i)}{\sigma_i} \quad (12)$$

where Z_i denotes a standard DI and $\bar{\beta}_i$ and σ_i are the mean and standard deviation of the DI, respectively. It should be noted that calculations of partial differential terms in strain energy, as shown in equation 8, are difficult. Therefore, in order to obtain precise results, the method of a cubic spline function is used to fit the values of the discrete mode shape. Moreover, the derivation and integration in equation (8) can be yielded by the fitted cubic spline function. In addition, the theoretical modal information of a beam before damage can be obtained through its analytical solution, and the theoretical MSE of the beam before damage then can be found.

Damage detection in beam structures

In order to simulate damages in a beam, bolted joints are used in this work. They can not only preset damage numbers and locations but also simulate different levels of looseness in bolted connections. Structures with bolted connections are widely used in civil engineering. Damage detection of these structures, such as looseness localizations for bolted joints, is an important research topic.^{17–20} A flowchart of damage detection of a beam with bolted joints used in this work is shown in Figure 1 according to the abovementioned theoretical methods. The arrangement of n DOFs with a uniform distribution for a cantilever beam is shown in Figure 2. In each setup of the experiment, three DOFs are tested and the second DOF is selected as a reference. Only

one-dimensional mode shapes (vertical direction) are considered here. Accelerometers are Kistler (8395A) with a sensitivity of 2000 mV/g and measurement range of $\pm 2g$. Environmental excitation is used to simulate random white noise. In order to obtain highly precise results, a sampling rate of 5000 Hz and total recording data length of 600 s were used in this study. The cantilever beam with a bolted joint is shown in Figure 3. Unless otherwise stated, the physical parameters of the cantilevers and clamped beams with single damage or multiple damages are listed in Table 1. The beam is made of low carbon steel.

The identified natural frequencies and corresponding standard deviations obtained by the BOMA method for cases I–IV in Table 1 are listed in Table 2. The measurements were conducted according to different measurement setups according to Figure 2. And the results in Table 3 show very good consistency for different setups.

Cantilever beam with different damages

Cantilever beams with single damage (case I with a single bolted joint) and multi-damages (case II with multi-bolted joints) were detected here. Figure 4 shows the first six identified mode shapes of the cantilever beam with a single bolted joint before and after damages obtained by the BOMA and theoretical method, respectively, where $\text{MAC} = |\varphi_i^T \varphi_i^*| / (\|\varphi_i\| \cdot \|\varphi_i^*\|)$; φ_i and φ_i^* are the i th mode shapes of the beam before and after damage, respectively. From the values of MAC in Figure 4, the difference of the mode shapes before and after damage is small. Thus, it is not reliable to locate

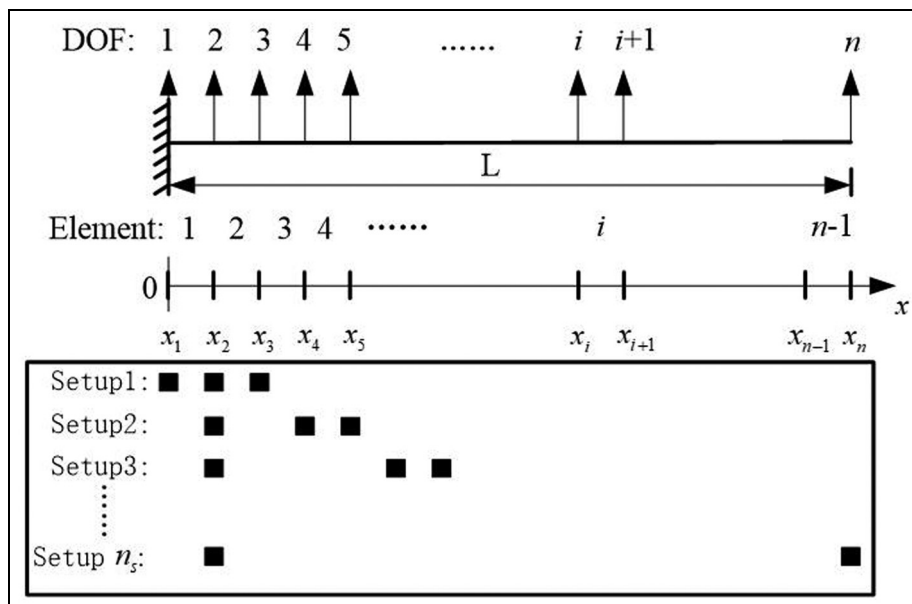


Figure 2. Arrangement of DOFs and measurement setups of the cantilever beam.

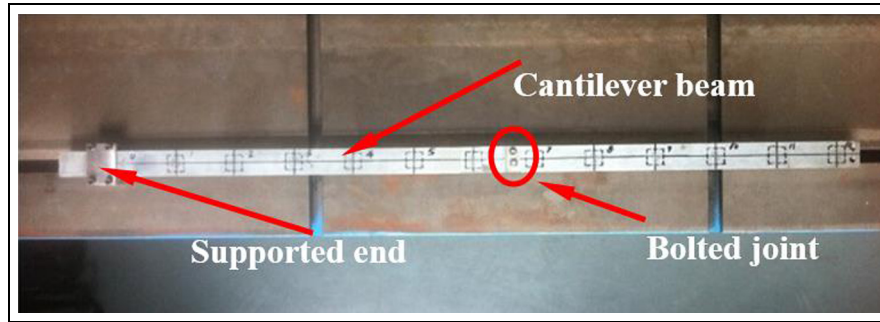


Figure 3. A single damage in the cantilever beam.

Table 1. Physical parameters.

| | Cantilever beam | | Clamped beam | |
|-----------------|----------------------|----------------------|-----------------------|----------------------|
| | Single-damage Case I | Multi-damage Case II | Multi-damage Case III | Multi-damage Case IV |
| Length (L/m) | 0.967 | 1.508 | 1.462 | 2.003 |
| DOFs (n) | 13 | 19 | 19 | 25 |
| Damaged element | 7 | 7, 13 | 7, 13 | 7, 13, 19 |

Table 2. Results of identified natural frequencies with different measurement setups (Unit: Hz).

| | | | Mode 1 | Mode 2 | Mode 3 | Mode 4 | Mode 5 | Mode 6 |
|--------------------------------------|--------------------|---------|--------|--------|--------|--------|--------|--------|
| Cantilever beam case I after damage | Frequency MPV | Setup 1 | 7.09 | 37.25 | 141.07 | 225.60 | 449.86 | 593.22 |
| | | Setup 2 | 6.99 | 35.39 | 141.21 | 225.35 | 447.11 | 584.52 |
| | | Setup 3 | 7.00 | 37.20 | 140.06 | 230.36 | 442.44 | 600.25 |
| | | Setup 4 | 6.66 | 36.36 | 139.97 | 227.45 | 436.52 | 595.35 |
| | Mean frequency | | 6.94 | 36.55 | 140.58 | 227.19 | 443.98 | 593.33 |
| | Standard deviation | | 0.19 | 0.87 | 0.65 | 2.31 | 5.84 | 6.57 |
| Cantilever beam case II after damage | Frequency MPV | Setup 1 | 3.00 | 17.83 | 44.83 | 111.62 | 169.80 | 229.35 |
| | | Setup 2 | 2.99 | 17.70 | 43.75 | 110.61 | 170.62 | 229.26 |
| | | Setup 3 | 3.00 | 17.48 | 44.29 | 111.32 | 170.51 | 229.46 |
| | | Setup 4 | 3.01 | 17.50 | 44.71 | 110.99 | 170.65 | 228.31 |
| | | Setup 5 | 2.97 | 17.91 | 44.80 | 111.01 | 170.83 | 232.78 |
| | | Setup 6 | 2.88 | 17.46 | 44.59 | 111.55 | 169.42 | 231.21 |
| Mean frequency | | 2.98 | 17.64 | 44.49 | 111.18 | 170.30 | 230.06 | |
| Standard deviation | | 0.05 | 0.20 | 0.41 | 0.38 | 0.56 | 1.63 | |
| Clamped beam case III after damage | Frequency MPV | Setup 1 | 22.74 | 55.76 | 124.08 | 194.73 | 263.61 | 421.57 |
| | | Setup 2 | 22.37 | 54.38 | 123.56 | 196.72 | 263.23 | 420.02 |
| | | Setup 3 | 22.06 | 55.64 | 123.07 | 197.55 | 263.81 | 416.44 |
| | | Setup 4 | 22.19 | 55.11 | 124.12 | 196.89 | 263.37 | 416.24 |
| | | Setup 5 | 22.55 | 54.85 | 122.32 | 196.89 | 263.87 | 418.42 |
| | | Setup 6 | 22.69 | 55.96 | 124.62 | 197.71 | 264.32 | 419.24 |
| Mean frequency | | 22.43 | 55.28 | 123.63 | 196.75 | 263.70 | 418.65 | |
| Standard deviation | | 0.27 | 0.61 | 0.83 | 1.07 | 0.39 | 2.07 | |
| Clamped beam case IV after damage | Frequency MPV | Setup 1 | 12.97 | 30.49 | 54.61 | 108.12 | 160.98 | 204.44 |
| | | Setup 2 | 12.92 | 30.10 | 53.55 | 107.43 | 161.69 | 205.55 |
| | | Setup 3 | 12.80 | 30.09 | 54.57 | 107.66 | 160.93 | 206.44 |
| | | Setup 4 | 12.72 | 30.45 | 54.30 | 107.57 | 161.55 | 206.09 |
| | | Setup 5 | 12.73 | 30.48 | 54.24 | 107.40 | 161.85 | 206.12 |
| | | Setup 6 | 12.82 | 29.90 | 54.57 | 107.86 | 161.06 | 205.63 |
| | | Setup 7 | 12.95 | 30.07 | 54.18 | 107.39 | 160.27 | 204.25 |
| | | Setup 8 | 12.99 | 30.58 | 54.86 | 108.59 | 161.56 | 205.22 |
| Mean frequency | | 12.86 | 30.27 | 54.36 | 107.75 | 161.24 | 205.47 | |
| Standard deviation | | 0.11 | 0.26 | 0.40 | 0.42 | 0.52 | 0.79 | |

MPV: most probable values.

Table 3. Contribution of individual modes to the damage index of the damaged element.

| Type | Element | Mode 1 (%) | Mode 2 (%) | Mode 3 (%) | Mode 4 (%) | Mode 5 (%) | Mode 6 (%) |
|--------------------|---------|------------|------------|------------|------------|------------|------------|
| Cantilever case I | 7th | 0.24 | 39.94 | 5.68 | 22.25 | 0.00 | 31.88 |
| Cantilever case II | 7th | 0.04 | 0.01 | 4.11 | 17.32 | 41.78 | 36.75 |
| | 13th | 0.10 | 0.01 | 38.03 | 26.71 | 2.27 | 32.88 |
| Clamped case III | 7th | 4.83 | 64.77 | 26.71 | 0.08 | 2.86 | 0.76 |
| | 13th | 1.11 | 7.06 | 85.50 | 0.34 | 5.68 | 0.30 |
| Clamped case IV | 7th | 11.47 | 17.91 | 11.31 | 5.64 | 45.66 | 8.00 |
| | 13th | 0.03 | 0.62 | 89.11 | 6.58 | 3.65 | 0.01 |
| | 19th | 1.48 | 5.03 | 28.30 | 64.91 | 0.28 | 0.00 |

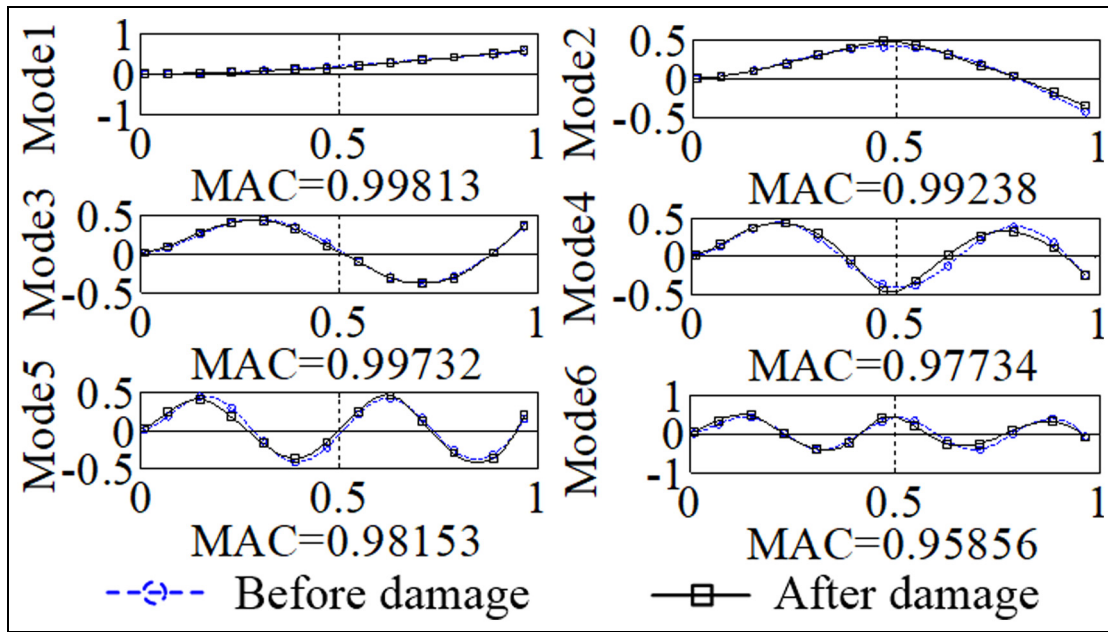


Figure 4. Mode shapes of the cantilever beam with a single bolted joint before and after damages (case I).

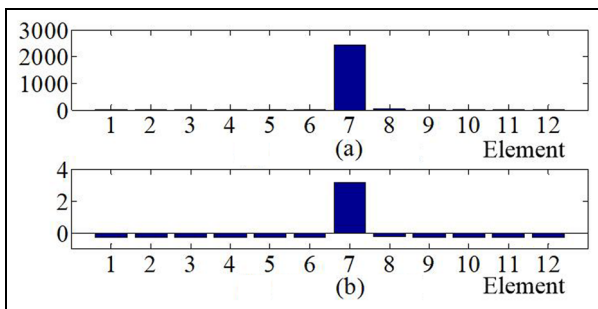


Figure 5. Element damage indices of the cantilever beam with a single bolted joint (case I): (a) damage index and (b) normalized DI.

the damage directly by the changes in mode shapes. Then, the DI is used to identify the location of the damage. The total and element MSEs can be calculated by

equations (7) and (8), and element damage indices can be obtained by equations (11) and (12) as shown in Figure 5. There is a peak in the 7th element of the cantilever beam, which simply reveals the damage location in accordance with the potential damage position. Figure 6 shows the first six identified mode shapes of the cantilever beam with two bolted joints before and after damages. The damage locations are in the 7th and 13th elements, which can be clearly seen in Figure 7 by the element damage indices. Thus, it is apparent that the element damage indices are suitable for detecting damage locations.

Clamped beam with different damages

Two clamped-clamped beams with different damages simulated by bolted joints were studied in this section. In case III, three beams were connected by two bolted

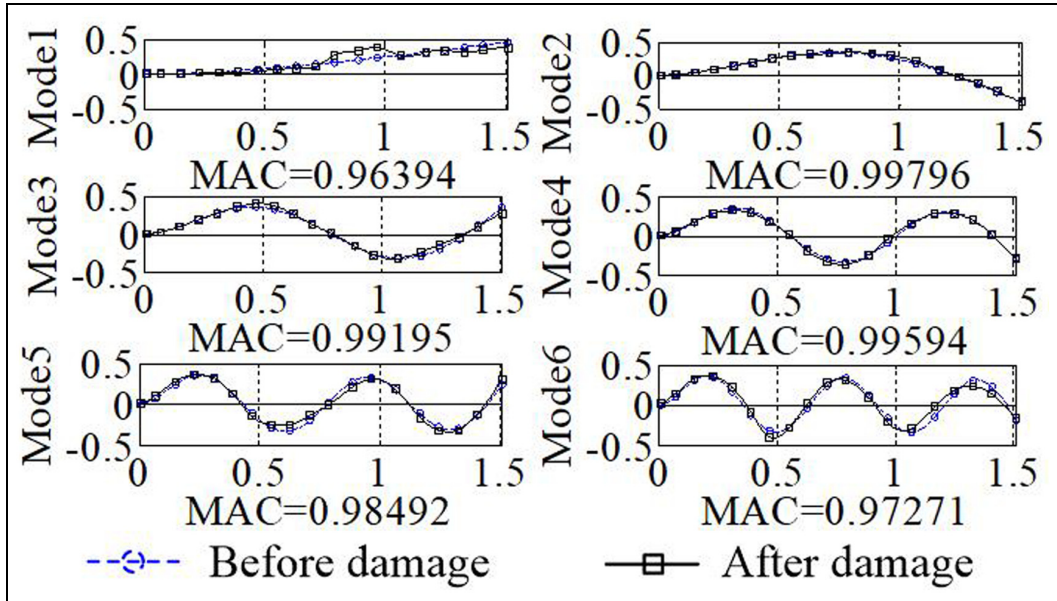


Figure 6. Mode shapes of the cantilever beams with two bolted joints before and after damages (case II).

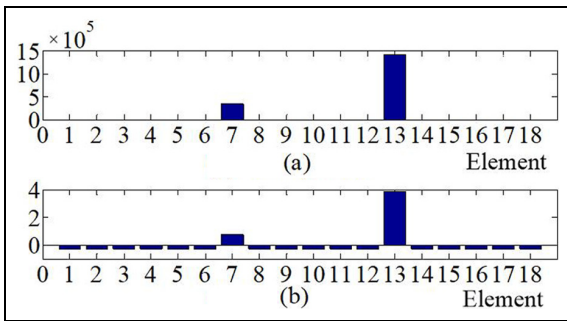


Figure 7. Element damage indices of the cantilever beam with two bolted joints: (a) damage index and (b) normalized DI.

joints. In case IV, three bolted joints connected four beams. Physical parameters and the damage locations of the two clamped-clamped beams are listed in Table 1. For case III, Figure 8 shows the first six identified mode shapes of the clamped-clamped beam with two bolted joints before and after damages obtained by the BOMA and theoretical method, respectively. Moreover, the element damage indices of the clamped-clamped beam in Figure 9 point out the damage locations successfully. For Case IV of the clamped-clamped beam with three damages, damage indices in Figure 10 can be used to identify the three damage locations even

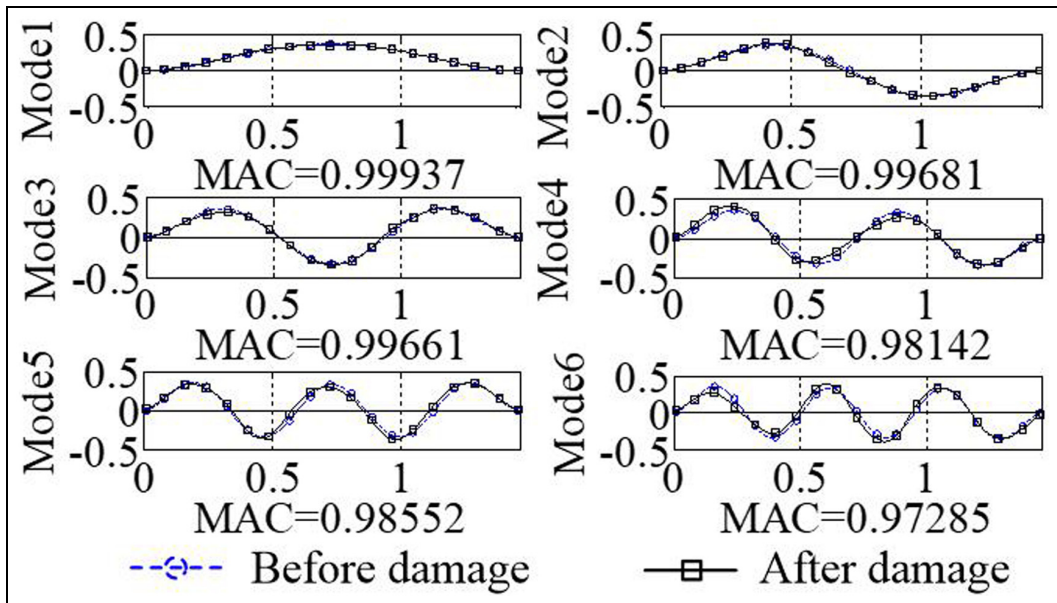


Figure 8. Mode shapes of the clamped-clamped beam with two bolted joints before and after damage (case III).

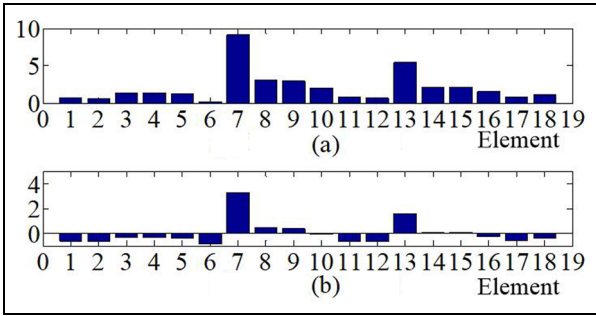


Figure 9. Element damage indices of the clamped-clamped beam (case III): (a) damage index and (b) normalized DI.

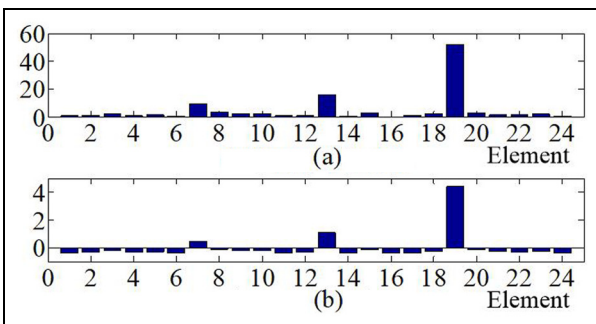


Figure 10. Element damage indices of the clamped beam (case IV): (a) damage index and (b) normalized DI.

if the MACs in Figure 11 are very close to 1. The results of the examination of the cantilever and clamped-clamped beams show that the values of DI of

the cantilever beams are much higher than those of the clamped-clamped beams, which indicate that cantilever beams are more sensitive to structural injuries. Contribution of individual modes to the DI of the damaged element is defined as $Z_{i,k}/Z_i \times 100\%$, where Z_i is a standard DI of the i th damaged element considered the effect of all the measured modes as shown in equation (12), and $Z_{i,k}$ is a standard DI of the i th damaged element only considered the effect of the k th measured mode. Table 3 listed the contributions of individual modes to the DI of the damaged element, from which one can find the following results: (1) the contributions of individual modes to the DI are related with locations of damages and boundary conditions of a beam; (2) the contribution of the first mode to the DI is relatively small.

Different looseness levels of bolted connections

DI was used to study different levels of looseness in the bolted connections of a cantilever beam with single damage and a clamped-clamped beam with multi-damages, as shown in Figure 12. Obviously, damage in Figure 12(b) is more severe than that in Figure 12(a), and hence, larger damage indices are expected. Figure 13(a) and (b) shows the DI for the cantilever and clamped-clamped beams, respectively. It can be found from Figure 13 that the damage increases with the increase in the looseness levels of the bolted connections and clearly the damage indices as well. Therefore, such methods indicate that there is a qualitatively proportional relationship between DI and damage levels.

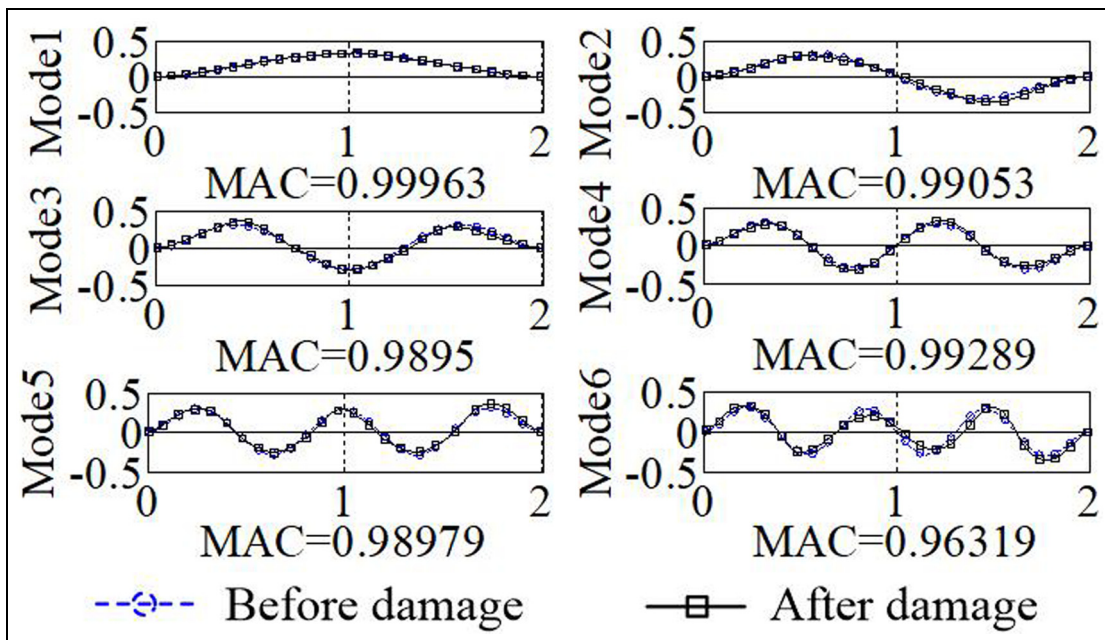


Figure 11. Mode shapes of the clamped-clamped beam with three bolted joints before and after damage (case IV).

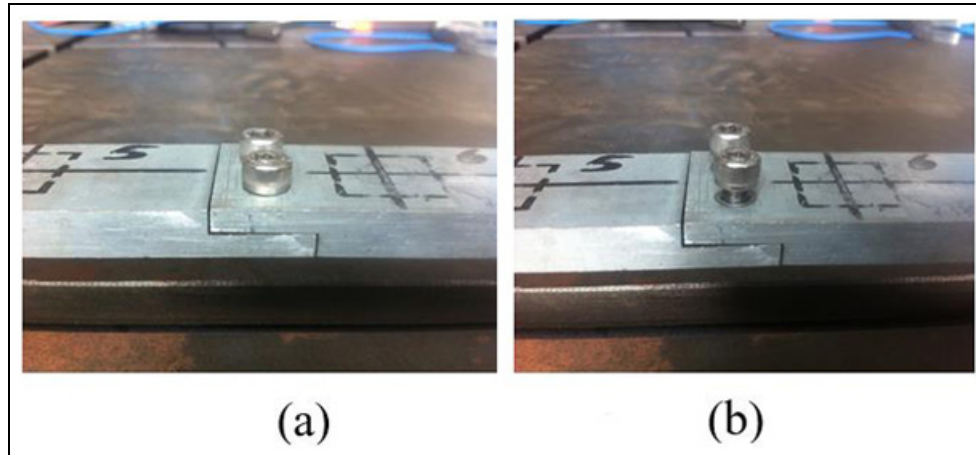


Figure 12. Arrangement of the different levels of looseness in the bolted connections: (a) damage level 1 and (b) damage level 2.

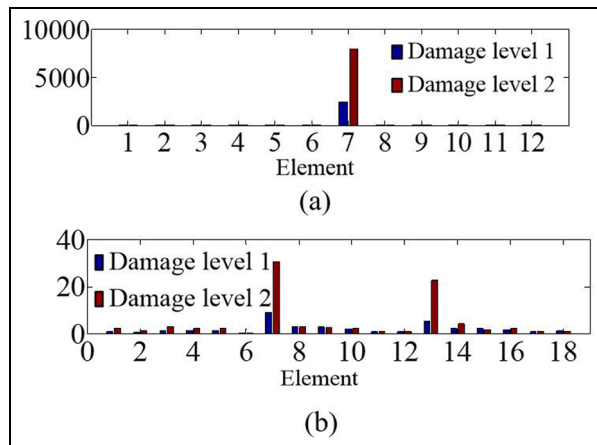


Figure 13. Comparison results of element damage indices with different damage levels for (a) the cantilever beam and (b) the clamped-clamped beam.

Conclusion

Using a non-destructive ambient vibration test, modal parameters of beam structures with different damages were identified by the BOMA method. One fundamental difference between the BOMA method and conventional approaches is that BOMA involves no concept of stochastic averaging and no decision on what quantity to average. Moreover, the BOMA and MSE methods can be used to identify locations and looseness of bolted joints in beam structures with different boundary conditions under ambient excitation. As applications, damage identification for beams with single damage or multiple damages under different boundary conditions (cantilever and clamped) were studied successfully by using a few mode shapes of beams only. Experiments for different levels of structural damages were carried

out, and comparison between DIs due to different looseness levels of the bolted connections demonstrated a qualitatively proportional relationship.

Declaration of conflicting interests

The author(s) declared no potential conflicts of interest with respect to the research, authorship, and/or publication of this article.

Funding

The author(s) disclosed receipt of the following financial support for the research, authorship, and/or publication of this article: The work described in this paper was fully supported by the grants from the Shanghai Natural Science Foundation (Grant No. 17ZR1419800) and the Shanghai Science and Technology Innovation Fund (Grant No. 17060502600).

ORCID iD

Cheng Jiang  <https://orcid.org/0000-0003-4688-5812>

References

1. Sun XD and Ou JP. Structural damage identification based on wavelet packet energy and PPCA. *Eng Mech* 2011; 28: 12–17.
2. Labib A, Kennedy D and Featherston C. Free vibration analysis of beams and frames with multiple cracks for damage detection. *J Sound Vib* 2014; 333: 4991–5003.
3. Yuen KV and Katafygiotis LS. Bayesian fast Fourier Transform approach for modal updating using ambient data. *Adv Struct Eng* 2003; 6: 81–95.
4. Au SK, Zhang F-L and Ni Y-C. Bayesian operational modal analysis: theory, computation, practice. *Comput Struct* 2013; 126: 3–14.
5. Au SK. Fast Bayesian FFT method for ambient modal identification with separated modes. *J Eng Mech* 2011; 137: 214–226.
6. Au SK. Assembling mode shapes by least squares. *Mech Syst Signal Pr* 2011; 25: 163–179.

7. Papadimitriou C and Papadioti DC. Component mode synthesis techniques for finite element model updating. *Comput Struct* 2013; 126: 15–28.
8. Zhang FL and Au SK. Fundamental two-stage formulation for Bayesian system identification, part II: application to ambient vibration data. *Mech Syst Signal Pr* 2016; 66–67: 43–61.
9. Jensen HA, Esse C, Araya V, et al. Implementation of an adaptive meta-model for Bayesian finite element model updating in time domain. *Reliab Eng Syst Safe* 2016; 160: 174–190.
10. Zhang FL, Ni YC and Lam HF. Bayesian structural model updating using ambient vibration data collected by multiple setups. *Struct Control Health Monit* 2017; 2412: e2023.
11. Zimmerman DC and Kaouk M. Structural damage detection using a minimum rank update theory. *J Sound Vib* 1994; 116: 222–231.
12. Li ZX, Yang XM and Ding Y. Damage identification neural network method based on statistical property of structural responses. *Eng Mech* 2007; 24: 1–7.
13. Naseralavi SS, Fadaee MJ and Salajegheh J. Subset solving algorithm: a novel sensitivity-based method for damage detection of structures. *Appl Math Model* 2011; 35: 2232–2252.
14. Hu MH, Tu ST, Xuan FZ, et al. Strain energy numerical technique for structural damage detection. *Appl Math Comput* 2012; 219: 2424–2431.
15. Hu HW, Wang BT, Lee CH, et al. Damage detection of surface cracks in composite laminates using modal analysis and strain energy method. *Compos Struct* 2006; 74: 399–405.
16. Shih HW, Thambiratnam DP and Chan THT. Vibration based structural damage detection in flexural members using multi-criteria approach. *J Sound Vib* 2009; 323: 645–661.
17. Doyle D, Zagrai A, Arritt B, et al. Damage detection in bolted space structures. *J Intel Mat Syst Struct* 2010; 21: 251–264.
18. Yang J, Xia Y and Loh CH. Damage identification of bolt connections in a steel frame. *J Struct Eng* 2014; 140: 04013064.
19. Blachowski B, Swiercz A, Gutkiewicz P, et al. Structural damage detectability using modal and ultrasonic approaches. *Measurement* 2016; 85: 210–221.
20. Pnevmatikos NG, Blachowski B, Hatzigeorgiou GD, et al. Wavelet analysis based damage localization in steel frames with bolted connections. *Smart Struct Syst* 2016; 18: 1189–1202.
21. Huang QD, Gardoni P and Hurlebaus S. A probabilistic damage detection approach using vibration-based non-destructive testing. *Struct Saf* 2012; 38: 11–21.
22. Gao WC, Liu W and Zou JX. Damage detection methods based on changes of vibration parameters: a summary review. *J Vib Shock* 2004; 23: 1–8.